JOURNAL OF Materials CHEMISTRY

Chemical synthesis of molybdenum disulfide nanoparticles in an organic solution

Dominique Duphil, Stéphane Bastide and Claude Lévy-Clément*

LCMTR, CNRS UPR 209, 2-8, rue Henri Dunant, 94320 Thiais, France.
E-mail: levy-clement@glvt-cnrs.fr

Received 4th March 2002, Accepted 13th May 2002
First published as an Advance Article on the web 14th June 2002

Molybdenum disulfide, MoS_2, nanoparticles can be synthesized either at high temperature as mono- and polycrystalline materials or at low temperature using various (electro)chemical routes. In the work presented, MoS_2 nanoparticles were obtained using a low temperature (140 °C) method *via* a chemical solution reaction route between the organometallic precursor $Mo(CO)_6$ and sulfur in *p*-xylene. As obtained, the MoS_2 nanoparticles of 10–30 nm diameter were mostly amorphous with a rounded shape. Upon annealing at 550 °C under vacuum, the nanoparticles lost their rounded shape and became slightly crystallized with curved (002) basal van der Waals planes (2H hexagonal structure). An increase of 2–4% in the $d_{(002)}$ spacing of the annealed MoS_2 nanoparticles compared to polycrystalline MoS_2 was observed. The size and shape of these nanoparticles play an important role for their properties, *e.g.* in catalysis and lubrication.

Introduction

Transition metal dichalcogenide MX_2 (M = Mo, W; X = S, Se) are semiconductor materials which exhibit a layered structure consisting of covalently bound X–M–X trilayers, separated by a relatively large van der Waals gap. The electronic structure is such that band-edge excitation corresponds largely to a metal centered d–d transition. Due to these features, the MX_2 compounds show numerous properties in the fields of catalysis, electrocatalysis, electrochemical intercalation and solid lubrication. They can be synthesized either at high temperature (800–900 °C) as mono- and polycrystalline materials[1] or at low temperature using various chemical routes[2–6] and electrochemical deposition.[7] Low temperature synthesis allows one to take advantage of some of the physical properties of solutions. For instance, multiphase systems can be used to form micelles for the growth of nanoparticles of many materials with controlled dimensions (*e.g.* MoS_2 synthesized in inverse micelles[3]). Several synthesis methods performed at low temperature can also offer some control over the nanoparticle characteristics. In the case of MoS_2, electrochemical deposition has been used to obtain thin films of well-ordered nanoclusters with their basal planes oriented perpendicular to the substrate[7] and MoS_2 fullerenes have also been produced using sonoelectrochemistry.[8] Depending on their size, these particles show unique properties not present in their corresponding poly- and monocrystalline phases. For example, highly nanostructured molybdenum disulfide, MoS_2, made by sonochemical synthesis catalyzes thiophene hydrodesulfurization with higher activities than those of the most active materials (*e.g.* RuS_2, $RuSe_2$).[5] The sonochemical synthesis is based on the irradiation of a slurry of molybdenum hexacarbonyl, $Mo(CO)_6$ and sulfur in an organic solvent with high intensity ultrasound under argon. In the present work, we show that the same $Mo(CO)_6$ and sulfur precursors can chemically react in xylene at 140 °C to give MoS_2 nanoparticles. Synthesis and characterization of the as-obtained and annealed at high temperature MoS_2 nanoparticles are reported in this paper.

Experimental

The synthesis was performed in *para*-xylene (bp 140 °C, Fluka no. 95685) with stirring and under a nitrogen atmosphere. Sulfur (99%, Prolabo, 7.3 mg, 2.3×10^{-4} mol) was added to the degassed (for 20 min) *p*-xylene solution (100 mL). The system was heated over a period of 30 min up to 140 °C to dissolve the sulfur, then cooled down to room temperature, maintaining nitrogen bubbling. $Mo(CO)_6$ (98%, Strem Chemicals) was added (30 mg, 1.15×10^{-4} mol) in such an amount that the S/Mo atomic ratio was 2. The temperature was raised to reflux (20 min) and maintained at 140 °C for several hours. The black–brown powder obtained was filtered and dried with acetone (Merck no. 310804).

MicroRaman spectroscopy was used to study the decomposition of the molybdenum hexacarbonyl during the reaction, using an Infinity spectrometer (Dilor Jobin-Yvon). The S/Mo concentration ratio in the powder was determined by Inductively Coupled Plasma with Atomic Energy Spectrometry (ICP/AES) analysis (Vista, Varian). ICP samples were prepared by dissolving the powder in aqua regia under sonification and diluting with ultrapure water (18.2 MΩ.cm). X-Ray diffraction (XRD) spectra were recorded using an automated Bruker D8Advance X-ray diffractometer, in the θ-2θ configuration with the CuK_α X-ray radiation. X-Ray spectra of the powder were corrected for the substrate holder background. High-resolution transmission electron microscopy (HRTEM) and selected area electron diffraction (SAED) analysis of the powder were performed using a Topcon 002B, to provide detailed examination of the nanostructure. EDX (Energy dispersive X-ray) spectra were recorded by using the Kevex EDX system model delta 5, attached to the Topcon. Specimens for TEM observation were prepared by briefly dispersing ultrasonically the MoS_2 powder in chloroform. The suspensions were allowed to stand for 2 min in order to let the largest particles settle out. One drop of the solution was then placed on a home-made copper grid covered by a polymer film coated with an evaporated amorphous carbon film. The copper grid was in contact with a filter paper to prevent particle agglomeration. Finally, the grid was dried at room temperature. All the high-resolution micrographs were taken at 200 kV at approximate Scherzer defocus.

Results and discussion

Synthesis

The progress of the chemical reaction in solution was followed by Raman spectroscopic analyses of test samples taken from

 DOI: 10.1039/b202162e

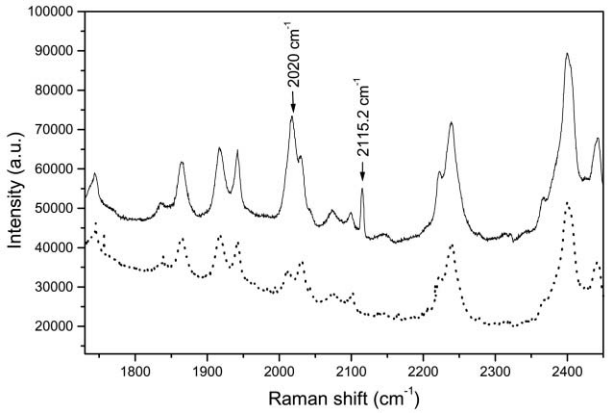

Fig. 1 Raman spectra of the *p*-xylene solution containing $Mo(CO)_6$ and sulfur, before the reaction (solid line), and after 120 min (dotted line) of reaction. The peaks of carbonyl groups are indicated by an arrow.

the bulk solution at different reaction times. The fraction of unreacted $Mo(CO)_6$ in solution was estimated from the band intensity of the A_{1g} vibration mode of complex carbonyl groups (2115 cm^{-1}), as shown in Fig. 1. Another band at 2020 cm^{-1} (E_g mode) was not considered as it was superposed with the vibration bands of the solvent (xylene). Free carbonyls that could remain in solution were not taken into account in this evaluation since the A_{1g} mode of free carbonyls occurs at higher frequencies (2155 cm^{-1}). Comparison of the spectra at different reaction times with the spectrum recorded before the start of the reaction showed that the intensity of the 2115 cm^{-1} band decreases, with no additional bands related to the formation of possible intermediate complexes. Fig. 2 gives the fraction of the unreacted $Mo(CO)_6$ in solution as a function of the reaction time. The consumption rate is lower during the early stages of the reaction because it takes 20 min to raise the temperature from the ambient ($t = 0$) to 140 °C. After 120 min, the 2115 cm^{-1} peak has disappeared, meaning that $Mo(CO)_6$ is no longer detectable. Concomitant to the consumption of $Mo(CO)_6$, the formation of a black powder is observed in the reaction vessel. Complementary experiments performed with $Mo(CO)_6$ only, or with selenium instead of sulfur, give similar consumption profiles, overall reaction time and formation of a black precipitate.

Characterization

As-obtained powder. ICP analysis of the brown–black powder gave a S/Mo atomic ratio in the range of 2.1–2.3.

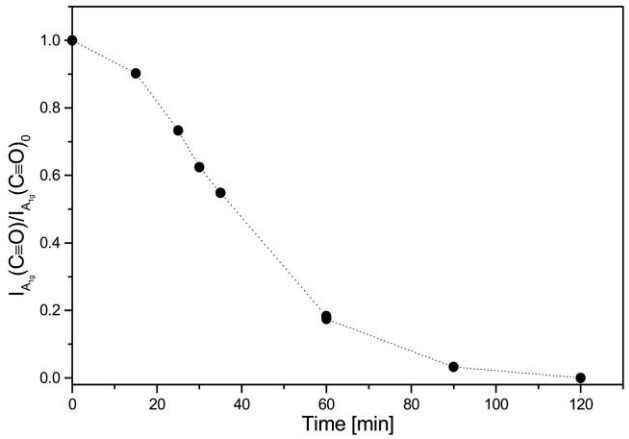

Fig. 2 Fraction of unreacted $Mo(CO)_6$ in *p*-xylene solution during the reaction with sulfur at 140 °C as a function of time. The ordinate axis represents the ratio between the intensities of the 2115 cm^{-1} A_{1g} vibration mode at different reaction times and at the initial stage.

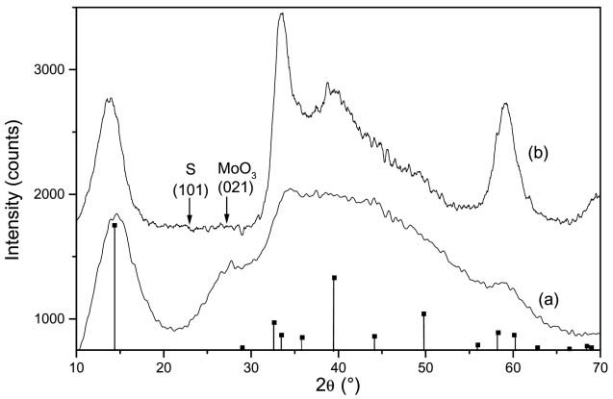

Fig. 3 XRD spectra of the MoS_2 powder. (a) as obtained; (b) annealed at 550 °C. The peaks of the 2H-MoS_2 structure are shown for comparison (ref. 10). The arrows indicate the (101) diffraction plane of S and (021) diffraction plane of MoO_3 (maximum intensities).

Within the accuracy of the ICP technique (~6%) this value indicates that the overall composition of the powder is MoS_2. The XRD spectrum (Fig. 3, spectrum a) exhibits one broad peak and a broad feature indicating the absence of crystalline long-range order. The overall spectrum is typical of amorphous MoS_2.[9] The broad peak centered at $2\theta = 14.6°$ corresponds to the (002) Bragg reflection of the hexagonal 2H-MoS_2 structure.[10] The broad feature between 20 and 70° could be the envelope of several peaks typical of the MoS_2 structure. The shoulder at 28° is attributed to molybdenum di- or trioxide.[11] No peak related to elemental sulfur is observed.

In order to understand the reaction mechanism of the formation of MoS_2, the black precipitate obtained by decomposition of $Mo(CO)_6$ at 140 °C in xylene (without sulfur) was characterized by XRD and HRTEM (not shown here). The XRD spectrum is indicative of an amorphous compound. A very broad peak centered at 28° is observed and attributed to molybdenum oxide impurities. HRTEM and electron diffraction confirm the amorphous character of the precipitate. From these results it is concluded that $Mo(CO)_6$, known to decompose at 150 °C in air,[12] is transformed into amorphous Mo at 140 °C in xylene. In contact with air or with some residual water present in the solvent, it may be oxidized, as no special care was taken to avoid contamination. These results suggest that, under our experimental conditions (140 °C), the overall reaction $Mo(CO)_6 + 2S \rightarrow MoS_2 + 6\ CO$ proceeds in xylene first through the formation of finely-divided, elemental Mo, which then reacts with S.

The HRTEM conventional bright field image in Fig. 4 reveals the morphological and nanostructural details of MoS_2. The powder is made up of well-defined, rounded and loosely connected nanoparticles with a fairly narrow size distribution (10–30 nm). The nanoparticles appear mostly amorphous but

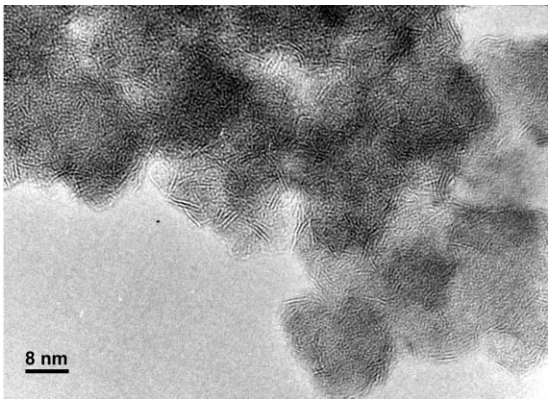

Fig. 4 HRTEM image of the nanostructure of the as-obtained MoS_2.

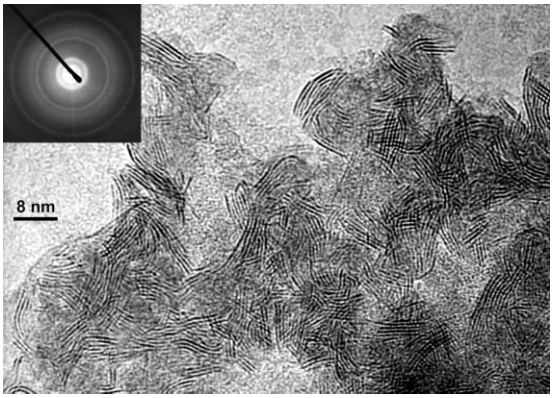

Fig. 5 HRTEM image of the nanostructure of the MoS_2 powder after annealing at 550 °C for 1 hour. In the inset is the corresponding SAED pattern.

some stacks of lattice fringes are observed with spacing in good agreement with the (002) van der Waals planes of bulk 2H-MoS_2 (0.616 nm). The SAED pattern consists of very diffuse diffraction rings, which confirms the amorphous nature of the as-obtained MoS_2.

Thermal annealing. In order to induce crystallization of the MoS_2 particles, the powder was annealed for 1 h at 550 °C in an evacuated sealed quartz tube. After annealing the MoS_2 powder maintains its black color. The X-ray diffraction spectrum shows that the broad peak attributed to molybdenum oxide (28°) disappears indicating that sublimation of oxide impurities occurs (Fig. 3, spectrum b). Broad peaks are observed at 33.5, 38.8 and 59.1°, which correspond to the (100), (103) and (110) planes of the 2H-MoS_2 structure, respectively. The apparition of the peaks indicates an enhancement of crystallinity in the sample. The shift of the (002) peak towards lower 2θ value suggests an increase of about 4% in the $d_{(002)}$ spacing along the c axis.

These results are confirmed by HRTEM observations and the SAED patterns (Fig. 5). Whereas the round shape of nanoparticles is not as well-defined as before annealing, a larger number of lattice fringes (corresponding to (002) planes) is observed. However, stacks of few lattice fringes never representing more than 10 MoS_2 layers, with typical dimension ranging between 20 and 40 nm can be seen, which is in agreement with the lack of long range order observed on the XRD spectrum. A $d_{(002)}$ spacing of 0.63 nm was measured from the respective SAED patterns. This value is larger by 2% than that of polycrystalline 2H-MoS_2 (d_{002} = 0.62 nm).[10] Furthermore, many planes are strongly bent. The increase of the d spacing may be interpreted as due to the curvature of adjacent MoS_2 planes linked by weak van der Waals forces. A similar increase in the d_{002} interlayer spacing was observed in MX_2 fullerenes which exhibit totally bent 002 planes leading to a closed structure.[13] Annealing at higher temperature (700 °C) does not improve significantly the crystallinity of the sample.

Conclusion

MoS_2 nanoparticles were obtained by a low temperature, chemical solution route using an organometallic precursor and sulfur. The reaction of $Mo(CO)_6$ and elemental sulfur in *p*-xylene under reflux produces a dark brown powder. ICP, XRD, and HRTEM analyses show that this powder is predominantly amorphous MoS_2 in the form of round nanoparticles. After annealing at 550 °C, HRTEM shows that somewhat-crystallized MoS_2 nanoparticles are obtained and that most of their basal (002) van der Waals planes are bent. However, in order to control the size and shape of the nanoparticles and produce materials suitable for applications in the fields of lubrication (fullerenes), electronics (nanotubes) or catalysis (nanostructured), the mechanisms of crystallization have to be further elucidated. Interesting new properties might be achieved and controlled that might prove helpful for the intended applications.

Acknowledgement

The authors thank G. Sagon of CNRS-LADIR (Thiais, France) for the Raman measurements, J.-C. Rouchaud of the CNRS-CECM (Vitry, France) for the ICP analysis and R. Tenne (Weizmann Institute, Israel) for the gift of microscopy grids.

References

1 *Preparation and crystal growth of materials with layered structures*, ed. R.M.A. Lieth, D. Reidel, Dordrech, Holland, 1977, **vol. 1**, p. 211.
2 D. Vollath and D. V. Szabo, *Mater. Lett.*, 1998, **35**, 236.
3 D. A. Rice, S. J. Hibble, M. J. Almond, K. A. H. Mohammad and S. P. Pearse, *J. Mater. Chem.*, 1998, **2**, 895.
4 J. P. Wilcoxon and G. A. Samara, *Phys. Rev. B.*, 1995, **51**, 7299.
5 M. M. Mdleleni, T. Hyeon and K. S. Suslick, *J. Am. Chem. Soc.*, 1998, **120**, 6189.
6 A. Albu-Yaron, C. Lévy-Clément, A. Katty, S. Bastide and R. Tenne, *Thin Solid Films*, 2000, **361–362**, 223.
7 S. Bastide, C. Lévy-Clément, A. Albu-Yaron, A-C. Boucher and N. Alonso-Vante, *Electrochem. Solid State Lett.*, 2000, **3**, 450.
8 Y. Mastai, M. Homyonfer, A. Gedanken and G. Hodes, *Adv. Mater.*, 1999, **12**, 1010.
9 R. R. Chianelli and M. B. Dines, *Inorg. Chem.*, 1978, **17**, 2759.
10 Powder Diffraction File 37-1492, PDF-2 Database Sets, International Center for Diffraction Data, Newton Square, PA, 1993.
11 Powder Diffraction Files 32-0671 and 05-0508, PDF-2 Database Sets, International Center for Diffraction Data, Newton Square, PA, 1993.
12 *Handbook of Chemistry and Physics*, CRC Press, Boca Raton, FL, 69th edn., 1988, p. B-108.
13 G. L. Frey, S. Elani, M. Homyonfer, Y. Feldman and R. Tenne, *Phys. Rev. B.*, 1998, **57**, 6666.